

Unified understanding of the breakdown of thermal mixing dynamic nuclear polarization: the role of temperature and radical concentration.

Ludovica M. Epasto,^{†,‡,||} Thibaud Maimbourg,^{II,‡} Alberto Rosso,^{*,§} and Dennis Kurzbach^{*,†,||}

[†]*University of Vienna, Faculty of Chemistry, Institute of Biological Chemistry, Währinger Straße 38, 1090 Vienna, Austria*

[‡]*These authors contributed equally to this work.*

^{II}*Université Paris-Saclay, CNRS, CEA, Institut de physique théorique, 91191, Gif-sur-Yvette, France*

[§]*Université Paris-Saclay, CNRS, LPTMS, 91405 Orsay, France*

^{||}*University of Vienna, Vienna Doctoral School in Chemistry (DoSChem), Währinger Str. 42, 1090 Vienna, Austria*

E-mail: alberto.rosso@u-psud.fr; dennis.kurzbach@univie.ac.at

Abstract

We reveal an interplay between temperature and radical concentration necessary to establish thermal mixing (TM) as an efficient dynamic nuclear polarization (DNP) mechanism. We conducted DNP experiments by hyperpolarizing widely used DNP samples, i.e., sodium pyruvate-1-¹³C in water/glycerol mixtures at varying nitroxide radical (TEMPOL) concentrations and microwave irradiation frequencies, measuring proton and carbon-13 spin temperatures. Using a cryogen consumption-free prototype-DNP apparatus, we could probe cryogenic temperatures between 1.5 and 6.5 K, i.e.,

below and above the flash point of liquid helium. We identify two mechanisms for the breakdown of TM: (i) Anderson type of quantum localization for low radical concentration, or (ii) quantum Zeno localization occurring at high temperature. This observation allowed us to reconcile the recent diverging observations regarding the relevance of TM as a DNP mechanism by proposing a unifying picture and, consequently, to find a trade-off between radical concentration and electron relaxation times, which offers a pathway to improve experimental DNP performance based on TM.

Introduction

Dynamic nuclear polarization (DNP) is one of the most versatile techniques to enhance the intrinsically low signal-to-noise ratios of nuclear magnetic resonance (NMR) signals.^{1,2} It has become increasingly popular owing to its wide applicability in solid-state NMR through magic angle spinning (MAS)-DNP at temperatures close to 100 K,³⁻⁶ and solution-state NMR⁷⁻⁹ or MRI¹⁰⁻¹² through dissolution DNP (DDNP) of ex-situ hyperpolarized samples below 2 K¹³⁻¹⁵ followed by rapid sample heating and transfer to an MRI scanner or NMR spectrometer. In DNP experiments, a sample containing paramagnetic centers (most frequently stable nitroxide or trityl radicals)^{16,17} is submitted to a high magnetic field and irradiated with microwaves that excite electronic transitions. As a result, the high electron polarization is transferred to the NMR-active nuclei surrounding the radicals, leading to an up to 10,000-fold¹³ signal boost in comparison to conventional NMR at ambient temperatures. The often-encountered concentration and acquisition-time limitations of conventional NMR spectroscopy can thus be partially overcome. Strikingly, despite the widespread use of DNP, the understanding of this non-equilibrium quantum process remains debated.

In the past decades, three main mechanisms were established to explain the electron-nuclear polarization transfer in frozen solids: the solid effect (SE), the cross effect (CE), and thermal mixing (TM). For the well-resolved SE,^{1,2,18} microwave irradiation induces

“forbidden” transitions in hyperfine-coupled two-spin systems composed of an electron and a nuclear spin, at microwave frequencies $\omega_{MW} = \omega_e \pm \omega_n$, where ω_e denotes the electronic Zeeman and ω_n the nuclear Zeeman gap. The CE^{19,20} is designed to explain DNP in samples containing bi-radicals with two populations of electron spins with Zeeman frequencies ω_{e1}, ω_{e2} . Under the resonance condition $\omega_{e1} = \omega_{e2} \pm \omega_n$, triple-spin-flip transitions transfer polarization between these electrons to nuclei, yielding nuclear polarizations of $P_n = (P_{e1} - P_{e2}) / (1 - P_{e1}P_{e2})$,^{19,21,22} with P_{e1}, P_{e2} the electronic polarizations. These transitions rely on electron-electron dipolar and electron-nuclear hyperfine interactions that induce mixing between the quantum states of the three spin species. For mono-radicals the CE is also important when the width of the electron paramagnetic resonance (EPR) line is larger than ω_n .²²

However, when the concentration of unpaired electrons becomes large enough, three-spin mixing events alone do not suffice to account for the hyperpolarization process. Instead, many-spin transitions must be considered, which lead to a coupling of the entire “bath” of electrons to the nuclei. In such a situation, a so-called thermal mixing (TM) of the spin species is assumed. This concept is based on the fact that the off-equilibrium quantum steady state of the electron spins is well described by two temperatures:^{1,23-27} the spin temperature T_s of the non-Zeeman reservoir and T_Z the temperature of the Zeeman reservoir. The nuclear species with Zeeman frequency below the non-Zeeman electronic energy scale will freeze at the same spin temperature as the electrons, T_s . The condition for strong nuclear hyperpolarization is then $T_s \ll T \ll T_Z$.

However, the experimental relevance of TM is still controversial. Its main fingerprint is the observation of a common spin temperature T_s for all the nuclear species of the sample ($^1\text{H}, ^{13}\text{C}, ^{14}\text{N}, \dots$).^{28,29} A second direct evidence of TM was demonstrated a long time ago by Atsarkin³⁰ on Ce^{3+} half-spin impurities in a CaWO_4 crystal devoid of nuclear spins (so that three-spin mixing processes are absent). He observed that the entire EPR profile is modified by microwave irradiation (including frequencies $\omega \neq \omega_{MW}$). The spectrum even

partially displayed an unusual reversal of polarization, an observation well compatible with a TM description by the two temperatures T_s , T_Z . Nonetheless, recent electron double resonance (ELDOR) experiments performed at various temperatures and radical concentrations challenged the relevance of TM³¹⁻³⁴ for experimental DNP. In particular, a large reorganization of the EPR spectrum was observed under irradiation but without any reversal of polarization. These measurements were explained not with TM but with a model combining the CE and a phenomenological spectral diffusion³¹⁻³⁴ (see also³⁵). Herein, we aim to resolve this discrepancy between these new results suggesting the absence of TM and the older direct observations of TM. For this purpose, we performed spin-temperature measurements under DNP of ^1H and ^{13}C nuclear spins varying both radical concentration and temperature. We observe a breakdown of TM under two conditions: either at high temperature ($T \gtrsim 5\text{-}10$ K) or at low radical concentrations. Consequently, TM is not a relevant mechanism for MAS-DNP that occurs around 100 K. It is instead the dominant regime for dissolution DNP (around 2 K) and controls the performance of the experiment. We rationalize these observations as a competition between the electron relaxation time and the time associated with spectral diffusion. Combining the present results together with earlier reports,³⁶ we propose a phase diagram that conciliates in a unified picture the above-mentioned experiments and indicates where efficient nuclear hyperpolarization by TM is expected.

Experimental section

DNP experiments were performed on a home-built cryogen consumption-free prototype based on a Cryogenic LTD cryostat-magnet combination described in Ref.³⁷ In brief, 1.5 M sodium pyruvate- $1\text{-}^{13}\text{C}$ were dissolved in freshly prepared solutions of varying TEMPOL (4-Hydroxy-2,2,6,6-tetramethylpiperidinyloxy) concentrations (40, 60, and 70 mM) in 50% v/v glycerol- d_8 , 40% D_2O , and 10% H_2O . 100 μL of each sample were then hyperpolarized

for 1.5 h at temperatures of 1.5, 3.5, 5 or 6.5 K, in a magnetic field of $B_0 = 6.7$ T employing 50 mW microwave irradiation. We used a Virginia Diodes microwave source coupled to a 16-fold frequency multiplier. For microwave sweep experiments the irradiation frequency was varied between 187.5 and 188.5 GHz. The maximum DNP efficiency for spin-temperature experiments was at 188.0 GHz. NMR signals were recorded every 5 s using 5° excitation angles obtained with radio frequency pulses at 285.3 MHz for ^1H or 71.3 MHz for ^{13}C , produced by a customized Bruker HDIII spectrometer console. For data analysis, the recorded signals were baseline corrected using polynomial fit functions and apodized using a Gaussian window function. The signals after Fourier transformation were then fitted to derive the signal amplitudes S . The resulting values were then extrapolated to infinite times using mono exponential growth functions.

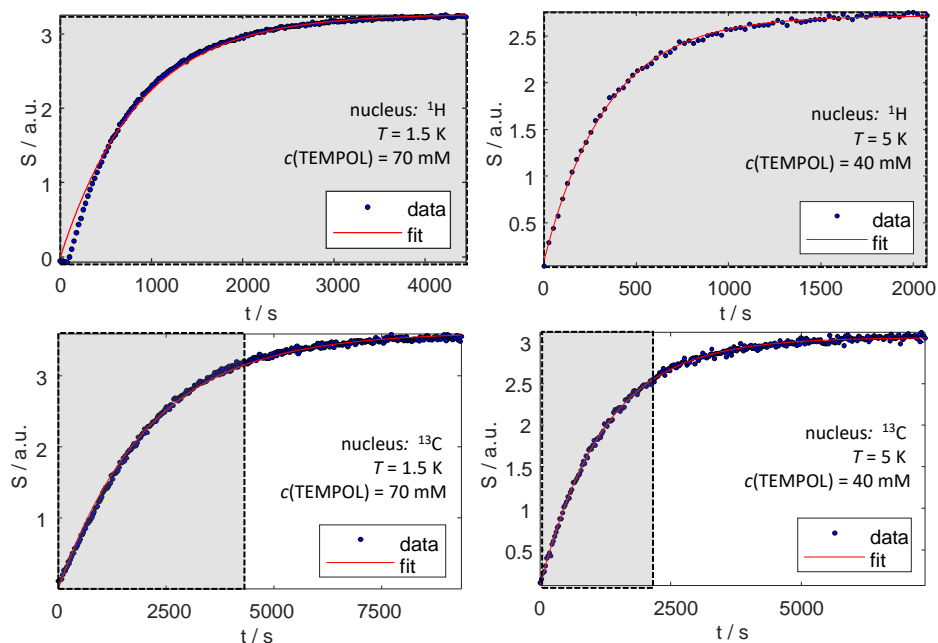


Figure 1: Signal build-up functions for two limiting cases: low radical concentrations and high temperature vs. high radical concentration and low temperature. In both cases, the build-up rates are different for proton and carbon-13 spins. The grey shades indicate equivalent periods of time.

Exemplary build-up curves and fits are shown in Fig. 1. The extrapolated signal

amplitudes at infinite times correspond to steady-state signal amplitudes. Hence, varying build-up rates did not influence our analysis.

Results

The signal amplitude S under irradiation is proportional to the nuclear polarization P_n . Hence, to determine the spin temperatures T_s through P_n , one needs to determine the proportionality constant in $S \propto P_n$. This is done by measuring the signal under off-resonance microwave irradiation of 187.52 GHz, i.e., in the absence of any DNP effect. There, the signal corresponds to the thermal equilibrium polarization $S_{\text{eq}} \propto P_{n,\text{eq}}$. As $P_{n,\text{eq}}$ is well known theoretically, P_n can be derived for generic irradiation frequency. For the spin temperature one then finds:

$$T_s = \frac{\hbar\omega_n}{2k_B \operatorname{arctanh}(P_n)} \quad (1)$$

The spin temperatures resulting from this procedure are shown in Fig. 2 for the herein-probed radical concentrations, temperatures, and nuclei, i.e., ^1H and ^{13}C . At high radical concentrations of 70 mM, both spin temperatures are compatible between 1.5 K and 5 K for both nuclei. In contrast, at lower concentrations of 40 mM TEMPOL, the spin temperatures never coincide. At 60 mM TEMPOL, the spin temperatures merge only below a temperature of 3.5 K. We interpret differing T_s values as a breakdown of TM. Hence, at high enough temperatures or low radical concentrations, the DNP process does not appear to be dominated by TM.

To further corroborate this interpretation and analyze the data obtained (especially at 70 mM) in more detail, we make use of the fact that the spin temperature is the only parameter in the hyperpolarization P_n that depends on the microwave frequency and that, when the spin temperature is not too small compared to the nucleus Zeeman gap, the

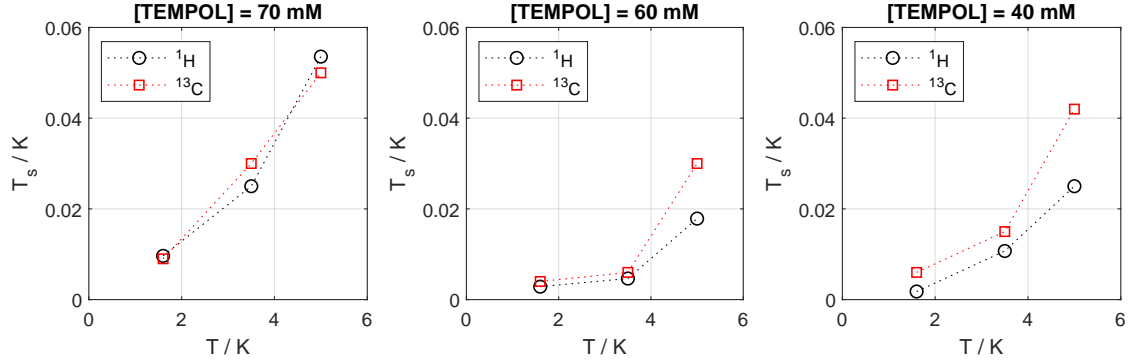


Figure 2: Spin temperatures T_S at long times with varying TEMPOL concentrations and sample temperatures T for ^1H and ^{13}C nuclei within the same sample. The points for 70 mM at 6.5 K are not reported because $P_{n,eq}$ is too small with respect to the noise.

relation between P_n and the spin temperature T_S becomes linear:

$$P_n = \tanh \frac{\hbar\omega_n}{2k_B T_S} \sim \frac{\hbar\omega_n}{2k_B T_S} \quad (2)$$

Therefore, when the spin temperatures of both species match, the signals as a function of the microwave frequency must display an identical shape.

In Fig. 3, we show the microwave sweep for each probed condition. We normalized the ^1H and ^{13}C profiles to their respective maxima. If thermal mixing holds, the obtained curves need to be identical, as both profiles rescale each other according to Eq. (2). Hence, we interpret a difference in these curves as a breakdown of TM. This method has the advantage that no thermal equilibrium signal intensity is required for referencing. Consequently, we manage to probe the breakdown of TM at TEMPOL concentrations of 70 mM at temperatures above 5 K, where the non-hyperpolarized signal intensities become prohibitively weak with our prototype setup.

At high TEMPOL concentrations of 70 mM, TM is present only below 6.5 K; at 60 mM, it starts to emerge below 5 K. Instead, for 40 mM, we have no sign of TM at any of the probed temperatures. Note that the reported signal amplitudes again correspond to

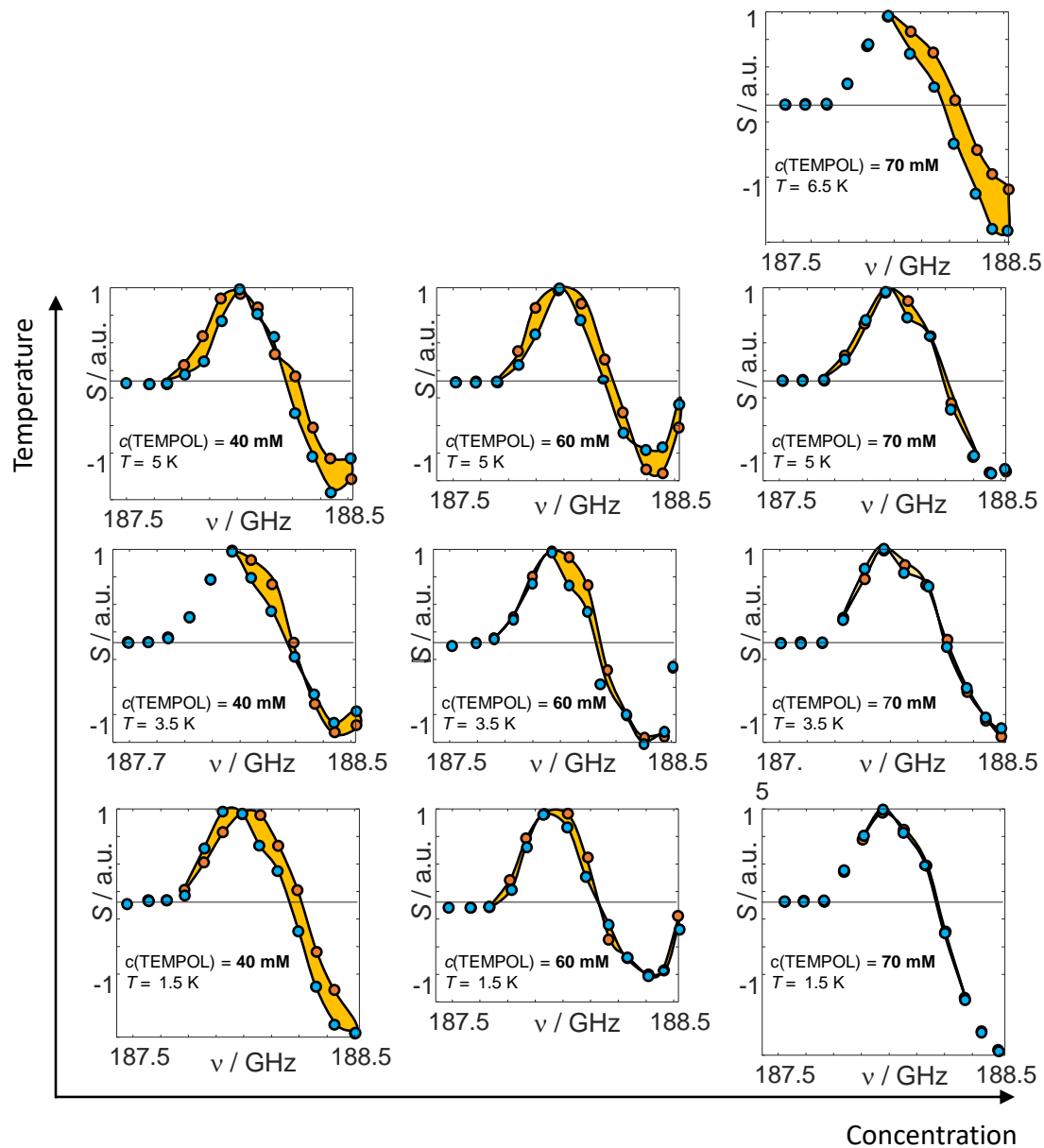


Figure 3: Signal intensities S in dependence of the microwave irradiation frequency ν for ^1H (blue) and ^{13}C (orange) spins for varying concentrations and temperatures. The yellow shades highlight the differences between proton and carbon profiles.

infinite build-up times. Interestingly, though, the build-up rate constants for ^1H and ^{13}C differ for all conditions probed herein (Fig. 1), even when spin temperatures converge

at long times. In the words of Wenckebach,² the probed TEMPOL-based radical system thus appears to transition into a regime of “slow” TM at increasing concentrations and decreasing temperatures.

Discussion

We propose a summary of our investigations in the diagram in Fig. 4 and discuss the hyperpolarization behavior and establishment of TM below.

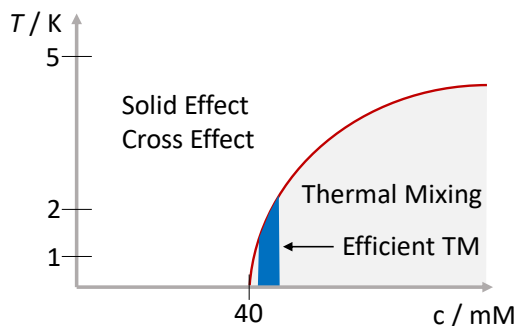


Figure 4: Phase diagram relating lattice temperature T and the radical concentration with different DNP regimes. For the samples probed herein, a maximum DNP efficiency was observed at the verge of TM breakdown, i.e., close to 40 mM.

The performance of a DNP protocol for hyperpolarizing nuclear spins can be quantified through the following formula for the nuclear polarization²¹

$$P_n = \frac{\int d\omega [P_e(\omega) - P_e(\omega + \omega_n)]}{\int d\omega [1 - P_e(\omega)P_e(\omega + \omega_n)]} \quad (3)$$

where $P_e(\omega)$ is the electronic polarization at frequency ω . This formula assumes an efficient polarization transfer through triple spin flips yet neglects nuclear relaxation processes with the lattice, as these are typically very slow (> 2 h at 1.4 K).³⁸ For simplicity, we assumed a rectangular EPR line for Eq. (3), as displayed in Fig. 5. However, it can be readily

generalized to arbitrary line shapes. Under microwave irradiation, the EPR spectrum is rearranged such that nuclear hyperpolarization arises from the imbalance of the electron polarizations $P_e(\omega) - P_e(\omega + \omega_n)$ in the numerator of Eq. (3). Three situations can occur: (i) Fig. 5 (top): homogeneous TM. When all electron spins are very rapidly mixed, the irradiated EPR line is uniformly reduced. As a result, the sample is poorly hyperpolarized. (ii) Fig. 5 (middle): inhomogeneous TM. In this regime, the electron spins are still mixed, yet the irradiated EPR line is asymmetric and displays the partial reversal of polarization as often observed in DNP applications. This is the best regime for nuclear hyperpolarization, as the imbalance of the electron polarizations $P_e(\omega) - P_e(\omega + \omega_n)$ accumulates. (iii) Fig. 5 (bottom): TM breaks down. Here the electron spins are not mixed. A spectral hole is “burnt” close to irradiation frequency. The imbalance changes sign across the irradiation frequency, implying a cancellation leading to weak or even negligible hyperpolarization.

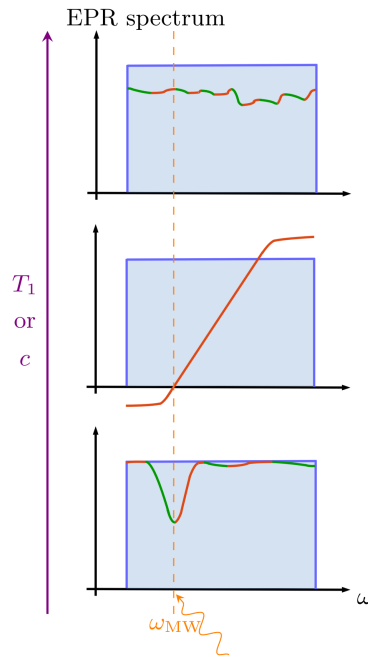


Figure 5: Sketches of the EPR spectra under irradiation at frequency ω_{MW} assuming varying electron relaxation times T_1 or radical concentrations c showing the cases of homogeneous TM (top), inhomogeneous TM (center), and TM breakdown (bottom). Red (resp. green) indicates frequency intervals in which the numerator’s integrand of Eq. (3) is negative (resp. positive). The blue line represents the equilibrium EPR line without any microwave irradiation.

Two control parameters allow one to switch from one regime to the other: the radical concentration c and the longitudinal electron relaxation time T_1 (itself temperature dependent,^{39,40} decreasing as temperature raises). These two handles have recently been established independently by Guarin et al.³⁶ and Maimbourg et al.²⁶ Taken together, these works suggest that high radical concentration or long relaxation times lead to homogeneous TM. On the contrary, if the radical concentration is too low or relaxation too fast, TM breaks down. As a consequence, the vademecum for a high nuclear hyperpolarization relies on the trade-off between radical concentration and relaxation time to induce inhomogeneous TM. Interestingly, at a given low temperature, the best performance has been observed at the verge of the TM breakdown in terms of radical concentration.³⁶

TM breakdown is a novel aspect of comprehending nuclear hyperpolarization at cryogenic temperatures. Interestingly, its two handles can be traced back to two different mechanisms of quantum localization. The first, à la Anderson, is obtained by decreasing the radical concentration and, thus, the strength of dipolar interactions against the disorder imposed by the g -factor anisotropy.^{41,42} Below a critical radical concentration, such disorder impedes the mixing of the eigenstates of the electron spin Hamiltonian.^{25,43} The second, à la Zeno, occurs when the single spin-flip transitions induced by the lattice are fast with respect to spectral diffusion. During these single spin flips, local operators such as S_i^+ , S_i^- , S_i^z act as measurements on the quantum state of the spins. When the rate of such quantum measurements becomes large enough, the quantum dynamics of the spectral diffusion are frozen²⁶ as in the quantum Zeno effect.^{44,45}

Conclusions

In conclusion, we have discovered that the efficiency of spectral diffusion, which underlies the effectiveness of TM in cases of heterogeneously broadened electron paramagnetic resonance (EPR) lines, depends not only on the radical concentration but also on the

experimental temperature. Assuming converging spin temperatures indicate the presence of thermal mixing (TM), our experimental data demonstrate that low sample temperatures and high enough radical concentrations favor TM as the predominant dynamic nuclear polarization (DNP) mechanism. Regarding the discrepancy between studies supporting TM as an efficient DNP mechanism and contradictory reports, our theory and data shed new light on this debate. The underlying studies have been conducted at different temperatures ranging from 1.2 to 20 K. It is thus highly likely that the diverging observations reported can be attributed to variations in the effectiveness of the quantum Zeno effect at different temperatures.

While it is intuitive to assume that increasing concentrations enhance the occurrence of electron flip-flop events that distribute information throughout the EPR spectrum, the temperature dependence is less apparent. However, considering that higher temperatures (and the resulting increased relaxation rates) lead to the occurrence of a quantum Zeno effect that freezes spectral diffusion processes, these dual conditions of TM efficiency become theoretically predictable and observed in our experiments. Our data demonstrate that an optimal hyperpolarization based on TM can be achieved at the crossover between TM and other mechanisms, such as the solid effect. This trade-off between radical concentration and electron relaxation times provides valuable insights into the controversy surrounding the predominance of TM as a DNP mechanism and may enhance existing DNP approaches to maximize nuclear polarization.

Acknowledgements

The authors thank the NMR core facility of the University of Vienna. We also thank Quentin M. Riedl, David O. Guarin, Denis M. Basko and Markus Holzmann. The project received funding from the European Research Council (ERC) under the European Union's Horizon 2020 research and innovation program (grant agreement 801936).

Conflicts of Interest

The authors declare no conflicts of interest.

References

- (1) Abragam, A.; Goldman, M. Principles of dynamic nuclear polarisation. *Reports on Progress in Physics* **1978**, *41*, 395.
- (2) Wenkebach, W. T. *Essentials of dynamic nuclear polarization*; Spindrift Publications, 2016.
- (3) Lesage, A.; Lelli, M.; Gajan, D.; Caporini, M. A.; Vitzthum, V.; Miéville, P.; Alauzun, J.; Roussey, A.; Thieuleux, C.; Mehdi, A., et al. Surface enhanced NMR spectroscopy by dynamic nuclear polarization. *Journal of the American Chemical Society* **2010**, *132*, 15459–15461.
- (4) Harrabi, R.; Halbritter, T.; Aussenac, F.; Dakhlaoui, O.; van Tol, J.; Damodaran, K. K.; Lee, D.; Paul, S.; Hediger, S.; Mentink-Vigier, F., et al. Highly efficient polarizing agents for MAS-DNP of proton-dense molecular solids. *Angewandte Chemie* **2022**, *134*, e202114103.
- (5) Alaniva, N.; Saliba, E. P.; Sesti, E. L.; Judge, P. T.; Barnes, A. B. Electron decoupling with chirped microwave pulses for rapid signal acquisition and electron saturation recovery. *Angewandte Chemie International Edition* **2019**, *58*, 7259–7262.
- (6) Berruyer, P.; Moutzouri, P.; Gericke, M.; Jakobi, D.; Bardet, M.; Heinze, T.; Karlson, L.; Schantz, S.; Emsley, L. Spatial Distribution of Functional Groups in Cellulose Ethers by DNP-Enhanced Solid-State NMR Spectroscopy. *Macromolecules* **2022**, *55*, 2952–2958.
- (7) Hilty, C.; Kurzbach, D.; Frydman, L. Hyperpolarized water as universal sensitivity booster in biomolecular NMR. *Nature protocols* **2022**, *17*, 1621–1657.

- (8) Otikovs, M.; Olsen, G. L.; Kupce, E.; Frydman, L. Natural abundance, single-scan ^{13}C - ^{13}C -based structural elucidations by dissolution DNP NMR. *Journal of the American Chemical Society* **2019**, *141*, 1857–1861.
- (9) Pinon, A. C.; Capozzi, A.; Ardenkjaer-Larsen, J. H. Hyperpolarization via dissolution dynamic nuclear polarization: new technological and methodological advances. *Magnetic Resonance Materials in Physics, Biology and Medicine* **2021**, *34*, 5–23.
- (10) Eichhorn, T. R.; Takado, Y.; Salameh, N.; Capozzi, A.; Cheng, T.; Hyacinthe, J.-N.; Mishkovsky, M.; Roussel, C.; Comment, A. Hyperpolarization without persistent radicals for in vivo real-time metabolic imaging. *Proceedings of the National Academy of Sciences* **2013**, *110*, 18064–18069.
- (11) Nelson, S. J.; Kurhanewicz, J.; Vigneron, D. B.; Larson, P. E.; Harzstark, A. L.; Ferrone, M.; Van Criekinge, M.; Chang, J. W.; Bok, R.; Park, I., et al. Metabolic imaging of patients with prostate cancer using hyperpolarized $[1-^{13}\text{C}]$ pyruvate. *Science translational medicine* **2013**, *5*, 198ra108–198ra108.
- (12) Comment, A. Dissolution DNP for in vivo preclinical studies. *Journal of Magnetic Resonance* **2016**, *264*, 39–48.
- (13) Ardenkjær-Larsen, J. H.; Fridlund, B.; Gram, A.; Hansson, G.; Hansson, L.; Lerche, M. H.; Servin, R.; Thaning, M.; Golman, K. Increase in signal-to-noise ratio of > 10,000 times in liquid-state NMR. *Proceedings of the National Academy of Sciences* **2003**, *100*, 10158–10163.
- (14) van Bentum, J.; van Meerten, B.; Sharma, M.; Kentgens, A. Perspectives on DNP-enhanced NMR spectroscopy in solutions. *Journal of Magnetic Resonance* **2016**, *264*, 59–67.
- (15) Köckenberger, W. Dissolution dynamic nuclear polarization. *eMagRes* **2007**, 161–170.

- (16) Kovtunov, K. V.; Pokochueva, E. V.; Salnikov, O. G.; Cousin, S. F.; Kurzbach, D.; Vuichoud, B.; Jannin, S.; Chekmenev, E. Y.; Goodson, B. M.; Barskiy, D. A., et al. Hyperpolarized NMR spectroscopy: d-DNP, PHIP, and SABRE techniques. *Chemistry–An Asian Journal* **2018**, *13*, 1857–1871.
- (17) El Daraï, T.; Jannin, S. Sample formulations for dissolution dynamic nuclear polarization. *Chemical Physics Reviews* **2021**, *2*.
- (18) Hovav, Y.; Feintuch, A.; Vega, S. Theoretical aspects of dynamic nuclear polarization in the solid state—the solid effect. *Journal of Magnetic Resonance* **2010**, *207*, 176–189.
- (19) Hwang, C. F.; Hill, D. A. Phenomenological model for the new effect in dynamic polarization. *Physical Review Letters* **1967**, *19*, 1011.
- (20) Hovav, Y.; Feintuch, A.; Vega, S. Theoretical aspects of dynamic nuclear polarization in the solid state—the cross effect. *Journal of Magnetic Resonance* **2012**, *214*, 29–41.
- (21) Serra, S. C.; Rosso, A.; Tedoldi, F. On the role of electron–nucleus contact and microwave saturation in thermal mixing DNP. *Physical Chemistry Chemical Physics* **2013**, *15*, 8416–8428.
- (22) Hovav, Y.; Shimon, D.; Kaminker, I.; Feintuch, A.; Goldfarb, D.; Vega, S. Effects of the electron polarization on dynamic nuclear polarization in solids. *Physical Chemistry Chemical Physics* **2015**, *17*, 6053–6065.
- (23) Provotorov, B. Magnetic resonance saturation in crystals. *Soviet Physics JETP-USSR* **1962**, *14*, 1126–1131.
- (24) Borghini, M. Spin-temperature model of nuclear dynamic polarization using free radicals. *Physical Review Letters* **1968**, *20*, 419.
- (25) De Luca, A.; Rosso, A. Dynamic nuclear polarization and the paradox of quantum thermalization. *Physical review letters* **2015**, *115*, 080401.

- (26) Maimbourg, T.; Basko, D. M.; Holzmann, M.; Rosso, A. Bath-induced Zeno localization in driven many-body quantum systems. *Physical Review Letters* **2021**, *126*, 120603.
- (27) Jähnig, F.; Himmler, A.; Kwiatkowski, G.; Däpp, A.; Hunkeler, A.; Kozerke, S.; Ernst, M. A spin-thermodynamic approach to characterize spin dynamics in TEMPO-based samples for dissolution DNP at 7 T field. *Journal of Magnetic Resonance* **2019**, *303*, 91–104.
- (28) Kurdzesau, F.; Van Den Brandt, B.; Comment, A.; Hautle, P.; Jannin, S.; Van Der Klink, J.; Konter, J. Dynamic nuclear polarization of small labelled molecules in frozen water–alcohol solutions. *Journal of Physics D: Applied Physics* **2008**, *41*, 155506.
- (29) Lumata, L.; Jindal, A. K.; Merritt, M. E.; Malloy, C. R.; Sherry, A. D.; Kovacs, Z. DNP by thermal mixing under optimized conditions yields > 60 000-fold enhancement of 89Y NMR signal. *Journal of the American Chemical Society* **2011**, *133*, 8673–8680.
- (30) Atsarkin, V. Verification of the spin-spin temperature concept in experiments on saturation of electron paramagnetic resonance. *Soviet Phys.-JETP* **1970**, *31*, 1012–1018.
- (31) Hovav, Y.; Kaminker, I.; Shimon, D.; Feintuch, A.; Goldfarb, D.; Vega, S. The electron depolarization during dynamic nuclear polarization: measurements and simulations. *Physical Chemistry Chemical Physics* **2015**, *17*, 226–244.
- (32) Kaminker, I.; Shimon, D.; Hovav, Y.; Feintuch, A.; Vega, S. Heteronuclear DNP of protons and deuterons with TEMPOL. *Physical Chemistry Chemical Physics* **2016**, *18*, 11017–11041.
- (33) Kundu, K.; Feintuch, A.; Vega, S. Electron–Electron Cross-Relaxation and Spectral Diffusion during Dynamic Nuclear Polarization Experiments on Solids. *The Journal of Physical Chemistry Letters* **2018**, *9*, 1793–1802.

- (34) Kundu, K.; Cohen, M. R.; Feintuch, A.; Goldfarb, D.; Vega, S. Experimental quantification of electron spectral-diffusion under static DNP conditions. *Physical Chemistry Chemical Physics* **2019**, *21*, 478–489.
- (35) Karabanov, A.; Kwiatkowski, G.; Perotto, C. U.; Wiśniewski, D.; McMaster, J.; Lesanovsky, I.; Köckenberger, W. Dynamic nuclear polarisation by thermal mixing: quantum theory and macroscopic simulations. *Phys. Chem. Chem. Phys.* **2016**, *18*, 30093–30104.
- (36) Guarin, D.; Marhabaie, S.; Rosso, A.; Abergel, D.; Bodenhausen, G.; Ivanov, K. L.; Kurzbach, D. Characterizing thermal mixing dynamic nuclear polarization via cross-talk between spin reservoirs. *The journal of physical chemistry letters* **2017**, *8*, 5531–5536.
- (37) Kress, T.; Che, K.; Epasto, L. M.; Kozak, F.; Negroni, M.; Olsen, G. L.; Selimovic, A.; Kurzbach, D. A novel sample handling system for dissolution dynamic nuclear polarization experiments. *Magnetic Resonance* **2021**, *2*, 387–394.
- (38) Negroni, M.; Turhan, E.; Kress, T.; Ceillier, M.; Jannin, S.; Kurzbach, D. Frémy's Salt as a Low-Persistence Hyperpolarization Agent: Efficient Dynamic Nuclear Polarization Plus Rapid Radical Scavenging. *Journal of the American Chemical Society* **2022**, *144*, 20680–20686.
- (39) Filibian, M.; Colombo Serra, S.; Moscardini, M.; Rosso, A.; Tedoldi, F.; Carretta, P. The role of the glassy dynamics and thermal mixing in the dynamic nuclear polarization and relaxation mechanisms of pyruvic acid. *Phys. Chem. Chem. Phys.* **2014**, *16*, 27025–27036.
- (40) Filibian, M.; Elisei, E.; Colombo Serra, S.; Rosso, A.; Tedoldi, F.; Cesàro, A.; Carretta, P. Nuclear magnetic resonance studies of DNP-ready trehalose obtained by solid state mechanochemical amorphization. *Phys. Chem. Chem. Phys.* **2016**, *18*, 16912–16920.

- (41) Anderson, P. W. Absence of diffusion in certain random lattices. *Physical review* **1958**, *109*, 1492.
- (42) Abanin, D. A.; Altman, E.; Bloch, I.; Serbyn, M. Colloquium: Many-body localization, thermalization, and entanglement. *Reviews of Modern Physics* **2019**, *91*, 021001.
- (43) Rodríguez-Arias, I.; Müller, M.; Rosso, A.; De Luca, A. Exactly solvable model for dynamic nuclear polarization. *Phys. Rev. B* **2018**, *98*, 224202.
- (44) Misra, B.; Sudarshan, E. G. The Zeno's paradox in quantum theory. *Journal of Mathematical Physics* **1977**, *18*, 756–763.
- (45) Facchi, P.; Pascazio, S. Quantum Zeno and inverse quantum Zeno effects. *Progress in Optics* **2001**, *42*, 147–218.